Acta Oceanol. Sin., 2024, Vol. 43, No. 6, P. 71–85
https://doi.org/10.1007/s13131-023-2308-9
http://www.aosocean.com
E-mail: ocean2@hyxb.org.cn

Effect of dissolved organic nitrogen on the bloom of *Prorocentrum donghaiense* and *Karenia* spp. in the East China Sea coastal waters

Xiaoru Cui[1, 2], Guangming Zhen[3], Jing Zhao[1]*, Keqiang Li[1, 3]*, Xiulin Wang[1, 3]

[1] Key Laboratory of Marine Chemistry Theory and Technology/Frontiers Science Center for Deep Ocean Multispheres and Earth System of Ministry of Education, Ocean University of China, Qingdao 266100, China

[2] College of Environmental Science and Engineering, Ocean University of China, Qingdao 266100, China

[3] College of Chemistry and Chemical Engineering, Ocean University of China, Qingdao 266100, China

Received 31 August 2023; accepted 15 January 2024

Abstract

Understanding the mechanism of harmful algal bloom formation is vital for effectively preventing algal bloom outbreaks in coastal environments. *Karenia* spp. blooms in the East China Sea show a significant correlation with nutrient regimes. However, the impact of key components of nutrients, especially dissolved organic nitrogen (DON), on the blooms of *Karenia* spp. is not clear. Quantitative research is still lacking. In this study, the cruise observations, field mesocosm-flask culture experiments, and a multinitrogen-tri-phytoplankton-detritus model (NTPD) are combined to reveal the quantitative influence of nutrient regimes on the shift of *Prorocentrum donghaiense* and *Karenia* spp. in the East China Sea. It has a synchronism rhythm of diatom-*P. donghaiense*-*Karenia* spp.-diatom loop in the field culture experiment, which is consistent with the results of the cruise observation. The results showed that the processes of terrigenous DON (TeDON) and dissolved inorganic nitrogen (DIN: NO_3^--N, NH_4^+-N) absorption promoted *P. donghaiense* to become the dominant algae in the community; whereas the processes of DON from *P. donghaiense* absorption promoted *Karenia* spp. to become the dominant algae in ambient DIN exhaustion. In addition, the three-dimensional fluorescence components of humus C, tyrosine and fulvic acid can indicate the processes of growth and extinction of *P. donghaiense* and *Karenia* spp., respectively. This study infers that *P. donghaiense* and *Karenia* spp. regime shift mechanism associated with the nutrient regime in coastal waters, which provides a scientific basis for the environmental management of coastal ecosystem health.

Key words: *Karenia* spp., *Prorocentrum donghaiense*, nutrients, multinitrogen-tri-phytoplankton-detritus model, three-dimensional fluorescence

Citation: Cui Xiaoru, Zhen Guangming, Zhao Jing, Li Keqiang, Wang Xiulin. 2024. Effect of dissolved organic nitrogen on the bloom of *Prorocentrum donghaiense* and *Karenia* spp. in the East China Sea coastal waters. Acta Oceanologica Sinica, 43(6): 71–85, doi: 10.1007/s13131-023-2308-9

1 Introduction

With the impact of human activities, excessive nutrients discharge into the sea can lead to eutrophication. Coastal eutrophication can result in a decline in biodiversity and is the main factor contributing to harmful algal bloom (HAB) outbreaks (Anderson et al., 2002; Imai et al., 2006; Heisler et al., 2008). The toxigenic dinoflagellate blooms of *Karenia* spp. in the Gulf of Mexico has been studied since the 1960s and is characterized by a long duration and significant harm to aquatic organisms (Steidinger, 2009). In recent decades, *Karenia* spp. blooms have frequently appeared in global near-shore waters. In China, *Karenia* spp. blooms have trended from south to north since 1998 in the Zhujiang River Estuary (Li et al., 2019), coastal waters of Fujian Province (Long and Du, 2005), Changjiang River Estuary (Zhou et al., 2006), coast of Zhejiang Province (Yao et al., 2007) and Bohai Sea (An et al., 2011). Among them, the typical species are *Karenia mikimotoi* (Chen et al., 2021), *Karenia brevis* (Wang et al., 2006) and *Karenia digitalis* (Cen et al., 2020). Therefore, it is essential to study the ecological and oceanographic mechanisms of the algal blooms of *Karenia* spp.

The coastal waters of Sansha Town in Fujian Province, China have been a critical monitoring area for HABs in the East China Sea since 1989, with an average number of algae cells in surface seawater reaching 10^6 cells/L (Zhao et al., 2021). According to the historical data, the peak HABs in the East China Sea were mainly concentrated in spring and summer, and the dominant algal species were *Prorocentrum donghaiense* and *Karenia* spp. Meanwhile, the dominant group of algal blooms in this area evolved from nontoxic diatoms to partially toxigenic dinoflagellates, which fits a historical pattern of bloom (Glibert and Burkholder, 2011; Yan and Zhou, 2004; Zhou et al., 2008). Some studies predicted that by the end of 21st century, the biomass of 70% of dinoflagellates in the East China Sea will increase and that of diatoms will decrease (Xiao et al., 2018). Toxigenic dinoflagellate

Foundation item: The National Natural Science Foundation of China under contract No. 42130403; the Fundamental Research Funds for the Central Universities under contract No. 202362003; the National Key Research & Development Program of China under contract No. 2017YFC1404300.

*Corresponding author, E-mail: zhaojing8095@ouc.edu.cn; likeqiang@ouc.edu.cn

blooms would become more frequent and intense, under uncontrolled conditions and threaten the marine ecological health of the East China Sea (Xiao et al., 2018a, 2018b; Wang et al., 2022).

Many studies on blooms focused on the nearshore region and ascribed blooms to rainfall, runoff and ground water (Hu et al., 2006; Brand and Compton, 2007; Medina et al., 2020). However, the outbreak and maintenance of HABs involve a series of complex biological and chemical processes, including nutrient preferences and competition, growth rates, species competition and mortality (Liu et al., 2001; Mulholland et al., 2006; Vargo et al., 2008; O'Neil and Heil, 2014; Tilney et al., 2019). For example, the cell density of *Karenia* spp. was significantly positively correlated with chlorophyll *a*, inorganic phosphorus, chemical oxygen demand (COD) and dissolved oxygen (DO), and negatively correlated with ammonia nitrogen (Killberg-Thoreson et al., 2014). It is crucial to study the growth characteristics, environmental factors, and other physiological and ecological mechanisms, as well as the impact of nutrients in controlling algal blooms.

The concentration level and structure of nutrients are the foundation for the occurrence and decline of *Karenia* spp. blooms (Zhao et al., 2020; Zhang et al., 2015). Heil et al. (2014) found that coastal eutrophication caused by the increased nutrient concentration in coastal waters was the main reason for the algal bloom of *Karenia breuis*. Generally, environmental conditions with low concentrations of dissolved inorganic nutrients (DIN) and high concentrations of dissolved organic nutrients (DON, DOP) are favorable for dinoflagellate growth (Antia et al., 1991; Jeong et al., 2017; Kwon et al., 2019; Park et al., 2022). It was found that DON and urea concentrations could be critical regulatory factors for the density of small nudidinodinates such as *Karenia* (Lai et al., 2011). Because *Karenia* had enhanced absorption and utilization capacity of urea, DON and DOP under eutrophication conditions (Wang, 2015; Xia, 2016). In addition, ammonia nitrogen may be the main nutrient controlling factor in the *Karenia* spp. blooms, especially *K. mikimotoi* (Zhao et al., 2020). HABs are known to be influenced by nutrient concentration levels and structures. However, the impact of key factors and processes of nutrients on the blooms of *Karenia* spp. remains unclear.

Eutrophication is usually the key driver of HABs. Although some studies have shown that *Karenia* spp. can sustain its growth or competitive growth by absorbing phagocytic DON or DOP, and the key components of the dissolved organic matter remain unclear. The quantitative influence of nutrients on *Karenia* spp. blooms, especially DON and DOP, has not been studied. Therefore, field culture experiments and field observations were carried out in the coastal waters of the East China Sea to investigate the effects of DON on the growth of *Karenia* spp., using algal culture water and sewage water as DON sources. In addition, a three-dimensional fluorescence spectrum was used to analyze the effects of different DOM components. Furthermore, a multinitrogen tri-algae biogeochemical model was constructed to clarify the driving impact of nutrients on the blooms of *Karenia* spp. This work will provide information on the healthy and sustainable development of coastal ecosystems.

2 Methods

2.1 *Study area and field cruise observation*

The cruise stations are located in the East China Sea coastal waters of Sansha Town (26°92′N, 120°22′E), Fujian Province, China, with an average water depth of 34.9 m (Fig. 1). In recent years, due to the tremendous impact of human activities, *P. donghaiense* and *Karenia* spp. blooms have caused considerable damage to cooccurring organisms due to oxygen depletion and potential ammonium toxicity for fish (Huang and Qi, 1997; Harrison et al., 2011), resulting in profound negative impacts on the local tourism, aquaculture and marine ecological environments. A total of nine times of HABs occurred in Fujian Province, which lasted 57 d and affected an area of 110.54 km^2 in 2019. Among them, there were three associated toxic HABs caused by *K. mikimotoi*, accounting for 23.97% of the total area of HABs (Fujian Provincial Department of Ocean and Fisheries, 2019).

Six cruises were conducted at 16 survey stations from April 25 to June 12, 2019, to observe the blooms of *P. donghaiense* and *Karenia* spp. in coastal waters of Sansha Town. From May 23 to May 29, 2019, *K. mikimotoi* and *P. donghaiense* blooms broke out in Sansha Town coastal waters. According to the field investigation results, the density of *Karenia* spp. and *Scrippsiella* sp. were 10^6 cells/L and 10^7 cells/L, respectively, and the abundance of *P. donghaiense* was 10^8 cells/L. The numerical changes in temperature, salinity and DO in Sansha Town from April 25 to June 11,

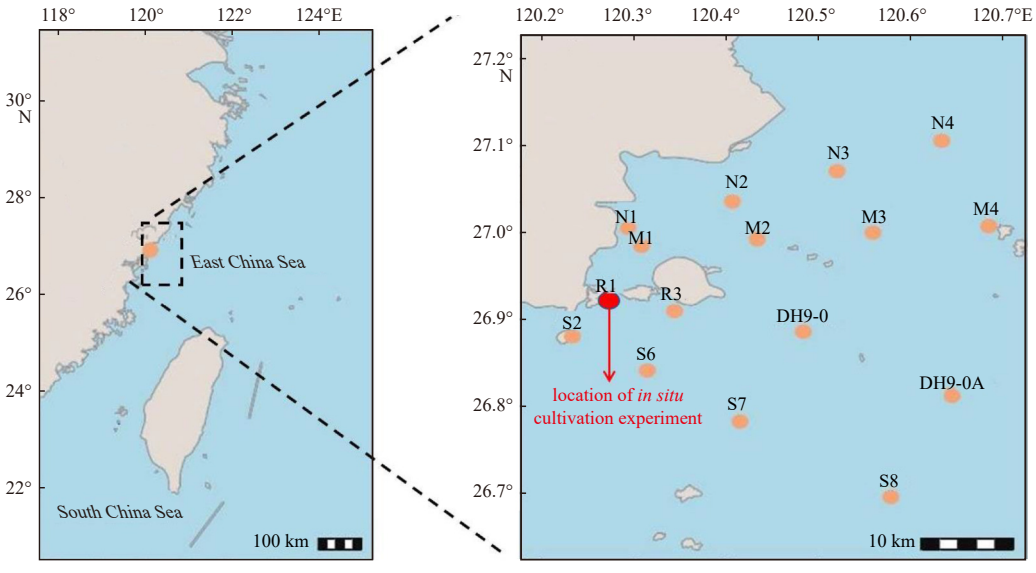

Fig. 1. Field cruise observation stations and mesocosm experiment site.

2019, were shown in Fig. S1.

2.2 *Field culture experiment*

The field mesocosm-flask culture experiments were performed on the fishing culture float shelf at the Station R1 (26°92.1′N, 120°27.1′E; Fig. 1) from June 6 to 16, 2019, where the seawater was collected at the time of the late stage of the algal bloom. The surface seawater was filtered by a 200 μm sieve (with zooplankton removed) to explore the effects of different sources of nutrients on the growth of phytoplankton. A 15 L PVC plastic bottle was filled with 10 L seawater, and the culture bottle was placed in the float shelf. The aim was to keep the temperature consistent with sea water and to simulate natural conditions as much as possible. We used three kinds of nitrogen nutrients (NO_3^--N, NH_4^+-N, DON) and PO_4^{3-}-P as the experimental groups and added NH_4^+-N at low concentrations and no nutrients as the DON control and blank, respectively. All groups were subjected to double disposal. Two kinds of DON were used: marine DON (MDON), taken from *P. donghaiense* culture water, and terrigenous DON (TeDON), taken from sewage treatment plants. The initial nutrient concentrations of the different enrichment groups are shown in Table 1, and the experimental apparatus is shown in Fig. 2.

The incubation period was 10 d, and samples were taken seven times: 0 d, 1 d, 2 d, 3 d, 4 d, 7 d and 9 d. The samples were taken regularly after each shake. The water sample was passed through 0.7 μm glass fiber filters (GF/F) immediately after collection. The filtrate was stored in four 40 mL brown glass vials for the determination of dissolved nutrients (NO_3^--N, NO_2^--N, NH_4^+-N, PO_4^{3-}-P, TDN, TDP), dissolved organic carbon (DOC) and colored dissolved organic matter (CDOM). The filter was wrapped in aluminum foil for the determination of PN (particle nitrogen)/PP (particle phosphorus) and Chl *a*. Except for CDOM samples, other samples were frozen at –20℃. All glass vials and filters used for collecting samples were combusted at 450℃ for 4 h. The values of temperature, DO, and pH were measured with a YSI (Professional Plus) and an illuminometer (LIHUADA, DT1332A) before sampling.

2.3 *Sample analysis method*

2.3.1 *Analysis methods of nutrients*

Nutrients of NH_4^+-N, NO_2^--N, NO_3^--N, and PO_4^{3-}-P were determined by a nutrient automatic analyzer (Bran-Lubbe Aiii, Germany) according to the method of Strickland and Parsons (1970). Seawater samples of TDN and TDP were oxidized by persulfate oxidation (120℃, 30 min) before they were determined using an autoanalyzer (Kwon et al., 2019). DON and DOP concentrations were calculated by subtracting inorganic nutrient concentrations from total dissolved nutrients (DON = TDN – DIN, DOP = TDP –

Table 1. Nutrient concentration (μmol·L^{-1}) setting for the field cultivation experiment

Number	Add	NH_4^+-N	NO_3^--N	NO_2^--N	DON	PN	PO_4^{3-}-P	DOP	PP
Blank group	/	1.34	5.84	1.07	32.85	7.95	0.21	0.42	1.71
Control group	NH_4^+-N	5.81	5.03	1.27	37.33	10.66	0.19	1.34	1.78
A	MDON	4.38	10.64	0.1	50.67	16.64	0.26	2.74	0.92
B	TeDON	3.91	10.79	1.78	42.43	16.26	0.23	2.51	1.18
C	PO_4^{3-}-P	3.87	7.45	0.47	35.21	16.87	1.29	1.34	1.76
D	NO_3^--N	3.87	34.61	0.47	35.21	16.83	0.28	1.30	1.71
E	NH_4^+-N	26.77	5.65	1.18	33.26	16.14	0.24	1.32	1.85

Note: The microalgae were filtered through a 0.45 μm glass fiber filter membrane in the blank group.

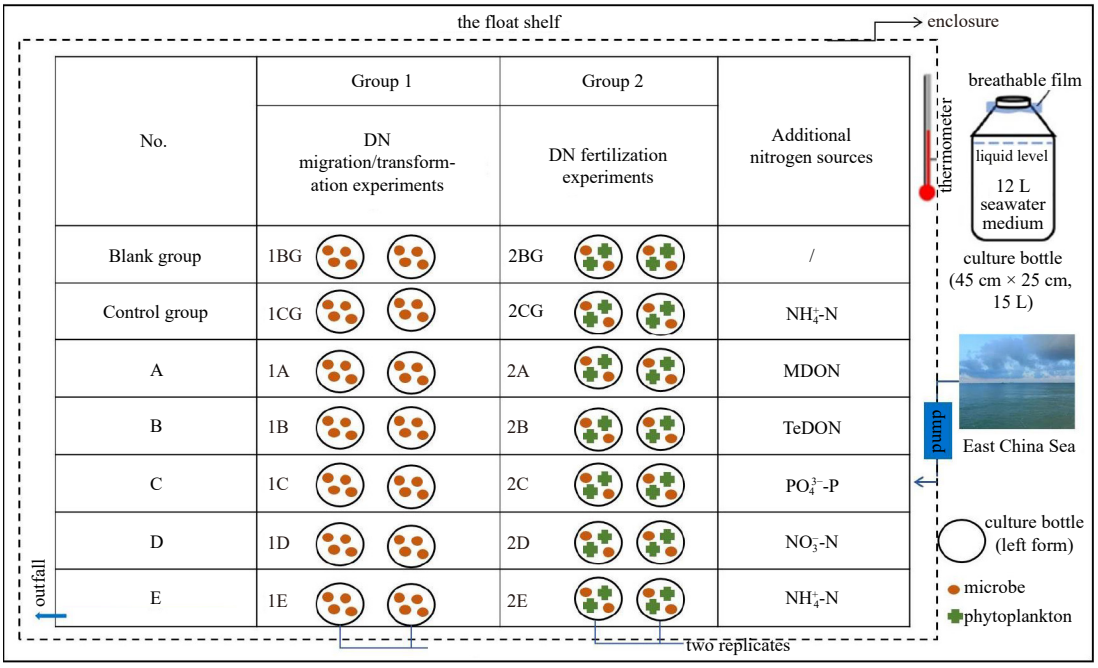

Fig. 2. Design of field mesocosm-flask culture experiment.

PO_4^{3-}-P). The filter samples of PP and PN were oxidized by persulfate oxidation (120℃, 30 min) and then determined using an autoanalyzer (Kwon et al., 2019). The DOC concentration was measured by high-temperature catalytic oxidation with an automatic analyzer (Multi N/C 3100, Germany).

2.3.2 *Method of Chl a and phytoplankton analysis*

The samples of Chl *a* were analyzed using a UV-Vis spectrophotometer (Optizen Alpha, Korea) after extraction with 90% acetone at 0℃ under dark conditions for 12–14 h (Parsons et al., 1984). The water samples of phytoplankton were fixed immediately after collection using Lugol's solution (20 g KI + 200 mL MQ water + 10 g I_2 + 20 mL acetic acid). Then the phytoplankton counting frame (0.1 mL) was utilized for identification and counting under an inverted microscope.

2.3.3 *Three-dimensional fluorescence spectrometry*

Fluorolog-3 (France-Jobin Yvon) was used to determine the emission excitation matrix (EEM) and three-dimensional fluorescence characteristics of the DOM samples (Massi et al., 2020). The composition and relative values of DOM in each sample were ultimately obtained by parallel factor analysis (Stedmon and Bro, 2008), which was performed using MATLAB software (MathWorks) with correction, descattering, and dearraying programs to analyze EEM.

2.4 *Model description*

The multinitrogen-tri-phytoplankton-detritus model (NTPD) was established using Modelmaker 4.0 (Cherwell Scientific Ltd., UK) to simulate the growth dynamics of three phytoplankton species. Based on the nutrient-biophytoplankton-detritus (NbPD) model (Chen et al., 2022), two dinoflagellates (*P. donghaiense* and *Karenia* spp.) and a diatom. In this model, the main environmental factors (e.g., temperature and light), nitrification and denitrification process equations of nutrients are consistent with the NbPD model (Chen et al., 2022).

The phytoplankton biomass in the field culture experiment was expressed as Chl *a* (μg/L) (Boyer et al., 2009; van de Poll et al., 2013). The biomass of the single species of algae (Bio_i) was estimated according to the Berger-Parker dominance index in cell density (DI_i) by the formula:

$$Bio_i = Bio_{total} \times DI_i \times R_{CC}, \quad (1)$$

where Bio_{total} is the total Chl *a* concentration, and we corrected DI_i from cell density to Chl *a* concentration by the ratio (R_{CC}) of Chl *a* concentration to algal cell (Tester et al., 2008; Lai et al., 2011). Other parameters in the model are shown in the Supporting Information (Table S1).

3 Results

3.1 *Changes in the phytoplankton community during the field cruise*

The *P. donghaiense* blooms broke out at stations N1–N4, M1–M4, R1, S2, and S8, with a cell density of 10^6 cells/L, whereas the

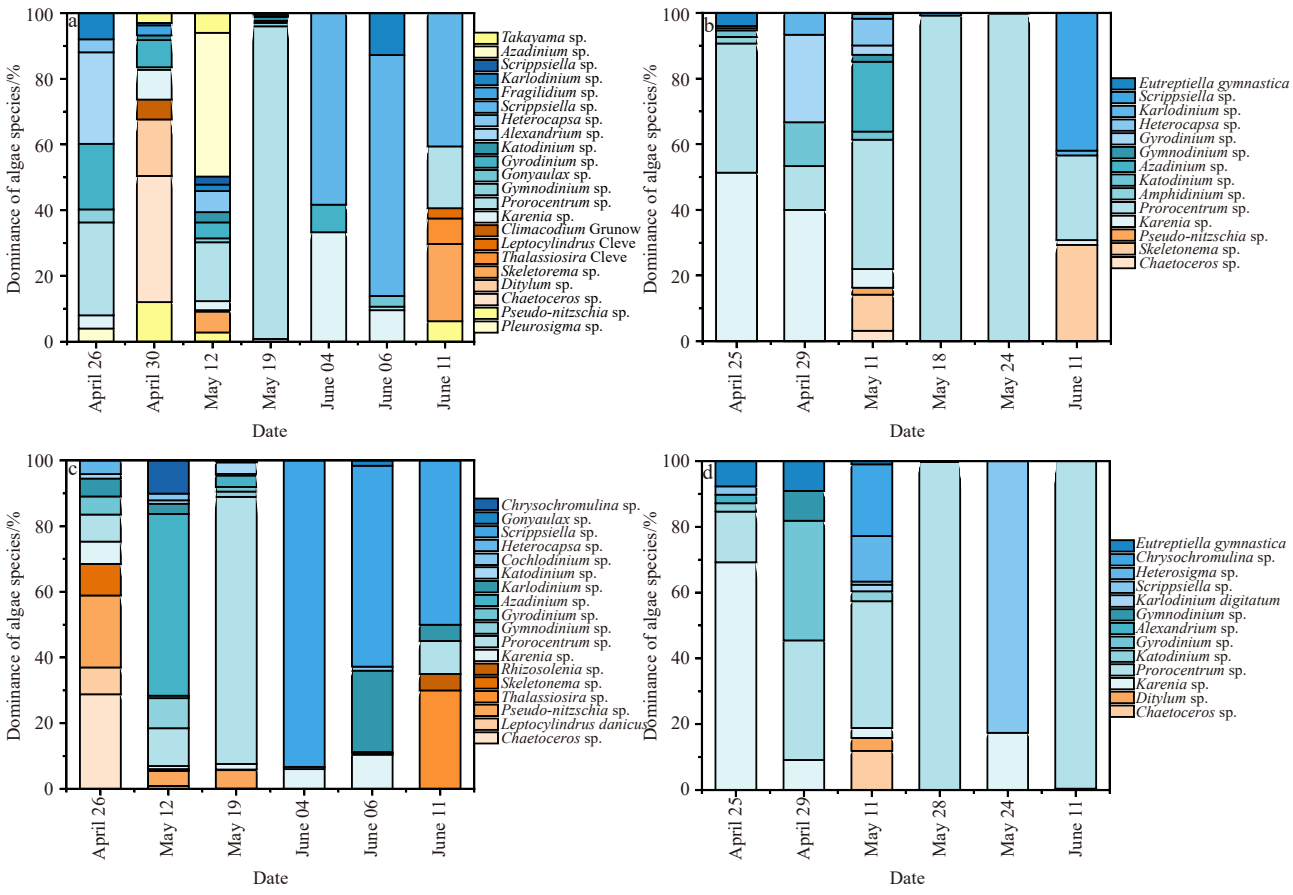

Fig. 3. Changes in the phytoplankton community in the field cruise stations of R1 (a), M1 (b), S2 (c), and N3 (d). Dominance of algal species is the Berger-Parker dominance index in cell density.

Karenia spp. blooms outbroke at the same stations except S8, with densities from 10^4 cells/L to 10^5 cells/L during the observation period from April to June 2019. These harmful algal blooms cause severe damage to the ecological environment of local coastal waters (Zhang et al., 2023; Lin et al., 2014, 2016). There is a synchronism rhythm of diatoms-*P. donghaiense-Karenia* spp.-diatom in which the phytoplankton regime shifts from diatoms to dinoflagellates of *P. donghaiense-Karenia* spp. loop (Fig. 3). The peak cell density of *Karenia* spp. reached 4.6×10^5 cells/L on June 4 after the peak cell density of *P. donghaiense*, which was 5.6×10^7 cells/L at Station R1 on May 19 (Fig. 3a). *Karenia* spp. can produce cytotoxins such as galactose and hemolysin, whose bloom outbreak (cell density > 10^4 cells/L) might cause ecological disasters and economic losses (Lv et al., 2019). The changes of Chl *a* at the four stations during field cruise observations are shown in Fig. S2. The concentration of Chl *a* ranged from 5.85 μg/L to 36.32 μg/L, and showed a trend of first increasing with peek value on May 18–19 and then decreasing.

3.2 *Spatial and temporal distribution of nutrients*

The significant changes in nutrients (DIN, DON, PO_4^{3-}-P) during field cruise observations are summarized in Fig. S3. The concentration of DIN ranged from 2.5 μmol/L to 36.0 μmol/L and gradually decreased over time. At the same time, the concentration of DON ranged from 2.0 μmol/L to 155.0 μmol/L and exhibited a trend of initially increasing and then decreasing. The rise in DON concentration was attributed partially due to terrestrial input and partially due to the mortality of phytoplankton such as *P. donghaiense*. The concentration of DON reached its maximum on May 18 and 19, 2019, and its descending order was R1, S2, M1 and N3. The trend in concentration variation trend of PO_4^{3-}-P was similar to that of DON. The decrease in PO_4^{3-}-P concentration might indirectly reflect the absorption and utilization of PO_4^{3-}-P by *K. mikimotoi*. The change in nutrient concentration was consistent with the loop in which the phytoplankton regime shifted from diatoms to dinoflagellates of *P. donghaiense-Karenia* spp. The high concentration of nutrients occurred in both western nearshore (R3, M2) and coastal areas (S8, DH9), which meant that terrigenous input and aquaculture sources coexist. Besides, the positive correlation between salinity and nutrients from the RDA (Fig. S4) results also indicated the existence of coastal aquaculture sources. These nutrient sources might support the occurrence of algal blooms in East China Sea coastal waters (Marques et al., 2024).

3.3 *Changes in phytoplankton biomass and community in the field culture experiment*

A total of 55 species of diatoms and 27 species of dinoflagellates were identified in the experimental period (Table S2). At the initial stage of the field experiment, there were four dominant dinoflagellates: *P. donghaiense*, *Scrippsiella trochooidea*, *K. mikimotoi*, and *Gonyaulax polygramma*, with dominance indices of 75%, 10%, 8%, and 3%, respectively (Fig. 4). *Prorocentrum donghaiense* was always dominant except in the MDON-supplemented culture group, and *K. mikimotoi* and *S. trochooidea* were dominant except diatoms in the MDON treatment group (Fig. 4a). Based on the concentration of Chl *a*, the phytoplankton biomass was significantly higher in the MDON and NO_3^--N addition culture groups than in the PO_4^{3-}-P, NH_4^+-N and TeDON treatment groups ($p < 0.05$) (Figs 4a–e). According to the Chl *a* content in algal cells of *P. donghaiense* and *K. mikimotoi* reported in the literature (Wang et al., 2006), the biomass in Chl *a* of *P. donghaiense* and *K. mikimotoi* was calculated (Figs 4a–e). *Karenia mikimotoi* increased in 0–4 d, and *P. donghaiense* decreased in the MDON group (Fig. 4a). Except for *P. donghaiense* and diatoms, *S. trochooidea* was replaced by *K. mikimotoi* in the PO_4^{3-}-P group (Fig. 4c). Generally, TeDON and DIN (NO_3^--N and NH_4^+-N) can promote the growth of *P. donghaiense*, and MDON and PO_4^{3-}-P might make *K. mikimotoi* more competitive.

3.4 *Changes in nutrients in the field culture experiment*

With the uptake and utilization of nutrients, phytoplankton grew during the first 4 d (exponential growth phase) as the concentration of PN increased in the field culture experiments (Fig. 5). The concentrations of NO_3^--N and NH_4^+-N decreased quickly during the first 2 d to 3 d in the MDON and TeDON adding groups, and the DON concentration then decreased until Day 7 during the later experimental phases (Figs 5a and b), which was associated with the growth of *Guinardia delicatula*, *P. donghaiense*, *S. trochooidea*, and *K. mikimotoi* (Figs 4a, b, f). The NO_3^--N and NH_4^+-N concentrations decreased during the first 4 days of the NO_3^--N and NH_4^+-N treatments (Figs 5d and e). With the exhaustion of nitrogen, *P. donghaiense* died rapidly (Figs 4d and e). NO_3^--N exhaustion, especially PO_4^{3-}-P addition, promoted the absorption of DON (Figs 5c and d), which might be the reason for the growth of *K. mikimotoi* in the later experimental phases (Figs 4c and d). In addition, the quantities of phosphate and DOP gradually decreased with the growth of phytoplankton (Fig. S5).

3.5 *Growth and nutrient uptake kinetics*

Based on the NTPD model, the growth and death processes of *P. donghaiense*, *K. mikimotoi*, and diatoms were well fitted (R^2 = 0.999 5 ± 0.270 5, $p < 0.05$), as shown in Fig. 6. The growth curve conforms to the logistic function, with maximum growth rates of 0.6 d^{-1} and 0.5 d^{-1} for *P. donghaiense* and *K. mikimotoi*, respectively. The growth of *P. donghaiense* under TeDON and DIN enrichment conditions had advantages. *Karenia mikimotoi* increased significantly in the enrichment of MDON and PO_4^{3-}-P.

The changes in nitrogen in the forms of NH_4^+-N, NO_3^--N, DON, PN and TN were also well simulated by the NTPD model (R^2 = 0.944 3 ± 0.073 2, $p < 0.05$) (Fig. 7). The concentration of TN in cultivation experiments was conserved, with a variation of less than 12%.

Some kinetic parameters associated with phytoplankton growth and nutrient uptake processes are shown in Table 2, and the other parameters are listed in the Table S1. A higher growth rate (K_G, 0.6 d^{-1}) with a quicker uptake rate of DIN (K_{up}–NH_4^+, 0.4 d^{-1}; K_{up}–NO_3^-, 0.5 d^{-1}) made *P. donghaiense* more competitive than *K. mikimotoi* and diatoms. However, a higher growth rate (K_G, 0.5 d^{-1}) with a quicker uptake rate of DON (K_{up}–DON, 0.3 d^{-1}) made *K. mikimotoi* more competitive than *P. donghaiense* in ambient MDON addition or DIN exhaustion. The DIN half-saturation (K_s) value of *K. mikimotoi* was higher than that of other algae, which might induce *K. mikimotoi* to bloom synchronously or after *P. donghaiense* and diatom blooms. This is consistent with the synchronism rhythm of the diatom-*P. donghaiense-Karenia* spp.-diatom loop in the field cruise.

3.6 *Three-dimensional fluorescence*

Based on the fluorescence intensity, there were three types of humus components including terrigenous humus C, fulvic acid and unknown substance N in the TeDON- added group. There

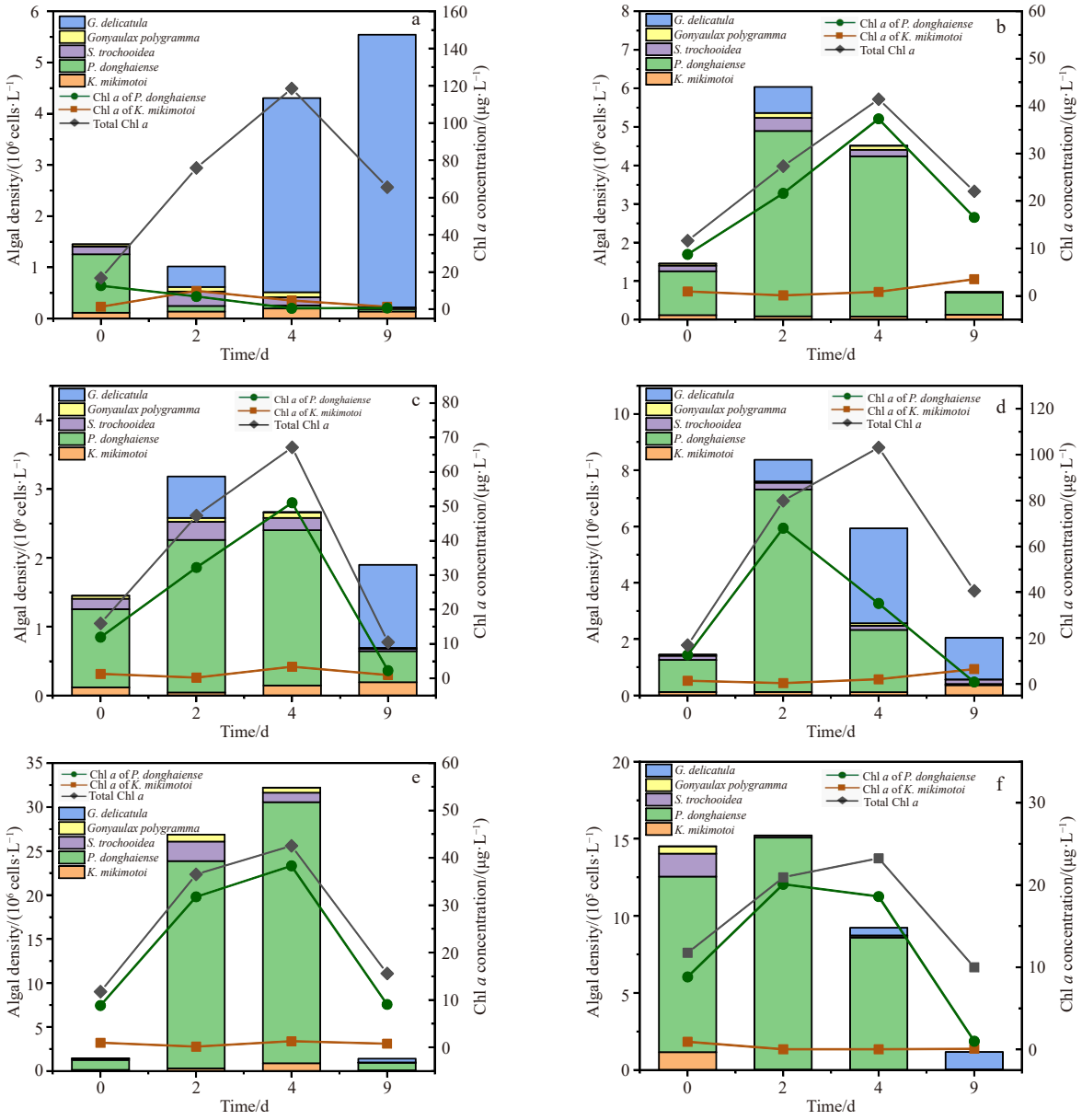

Fig. 4. The density of algal species and algae was predominant in the five groups with different source nutrients (a. MDON, b. TeDON, c. PO_4^{3-}-P, d. NO_3^--N, e. NH_4^+-N, f. control group).

were four types of components consisting of three types of humus (terrestrial humus C, marine humus and fulvic acid) and one type of protein (tyrosine) in the other nutrient-addition groups (Fig. 8).

The cell density of *K. mikimotoi* and *G. delicatula* were consistent with the fluorescence intensity fluctuation of the fulvic acid component with the decrease in DON concentration in the MDON and PO_4^{3-}-P treatment groups (Figs 8a and c), while there was little correlation ($p > 0.5$) between the cell density of *G. delicatula* and the fluorescence intensity of the fulvic acid component in the NO_3^--N treatment group. This might imply that the growth of *K. mikimotoi* might be promoted by DON with a fulvic acid component in the MDON and PO_4^{3-}-P treatment groups. The cell density of *P. donghaiense* was consistent with the fluorescence intensity fluctuation of terrestrial humus C and marine humus components with the decrease in DON concentration in the TeDON and NO_3^--N treatment groups and consistent with the fluorescence intensity fluctuation of the tyrosine component with the decrease in DON concentration in the NH_4^+-N treatment group (Figs 8b, d and e). The fluorescence results of both field culture experiments were consistent with the field observation (Fig. S7), which showed that *K. mikimotoi* was related to the fulvic acid component, and *P. donghaiense* was related to the terrestrial humus C, marine humus and tyrosine components.

To further verify the relationship between three-dimensional fluorescence components and phytoplankton growth and extinction, the Monte Carlo method was used in MATLAB to conduct correlation analysis. The correlation analysis results are shown in Fig. 9. The absolute value of the number is close to 1, indicating a stronger correlation. The results showed that the growth of *K. mikimotoi* was related to fulvic acid (0.767 5 ± 0.287 5) and *P. donghaiense* (0.752 ± 0.228). The correlations between *P. donghaiense* and terrigenous humus C and tyrosine were 0.593 3 ± 0.113 3 and 0.582 5 ± 0.292 5, respectively.

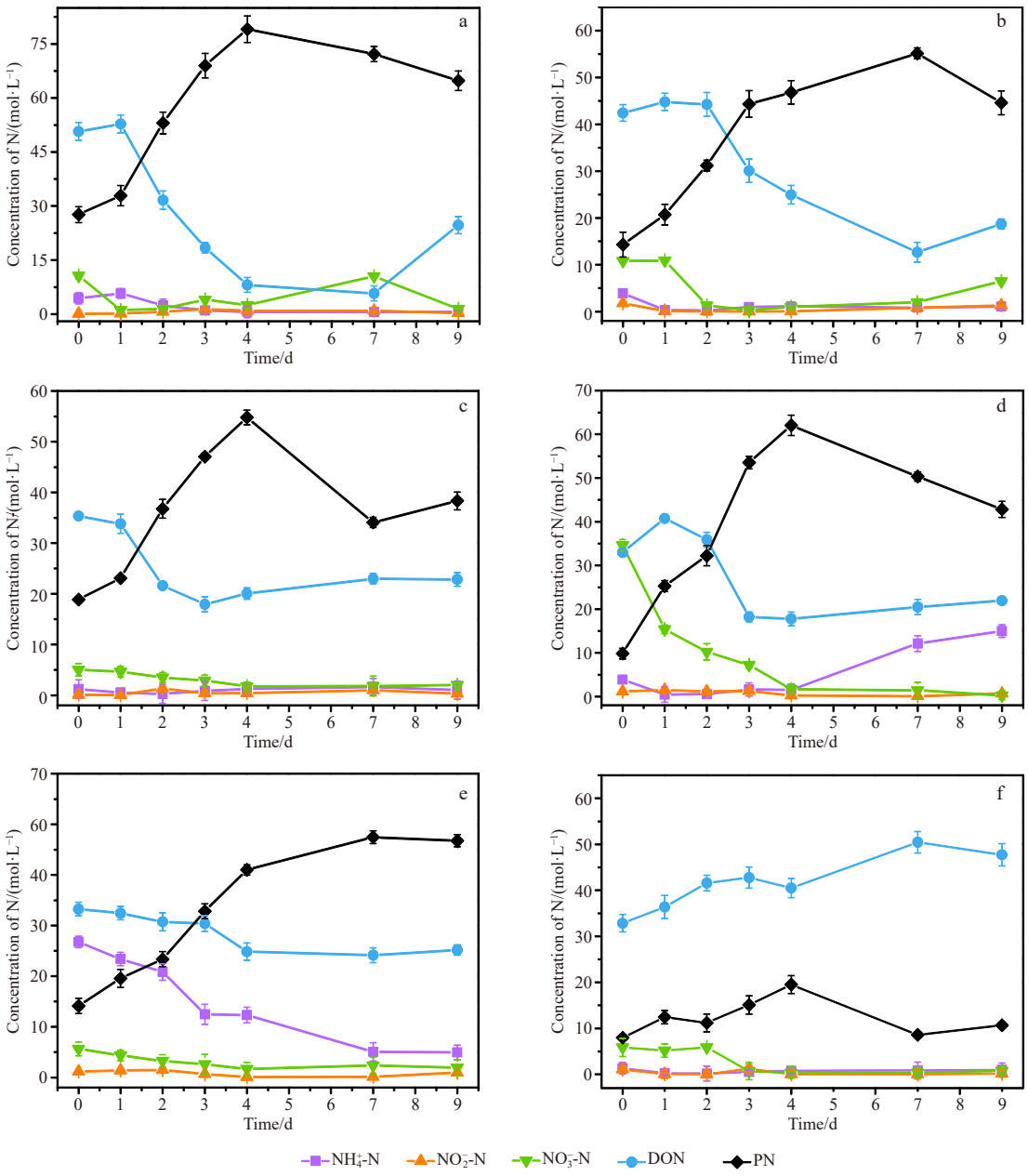

Fig. 5. Concentration changes of different N forms in the field culture experiments (a. MDON, b. TeDON, c. PO_4^{3-}-P, d. NO_3^--N, e. NH_4^+-N, f. control group).

4 Discussion

4.1 *Nutrient mechanism on the blooms of P. donghaiense and Karenia spp.*

Nutrient structure is one of the main factors affecting phytoplankton abundance and dominant species (Mathew et al., 2021). From the perspective of nutrient structure, dinoflagellates can directly absorb and utilize DON and DOP (Huang et al., 2005; Xiao et al., 2019; Wang et al., 2021). According to the field culture experiments, *P. donghaiense* absorbed DIN faster with a lower K_s of DON than *K. mikimotoi* (Table 2), which was more conducive to its growth process. Nutrients such as DON released by the *P. donghaiense* cells could serve as nutrients to maintain the *Karenia* bloom. *Karenia mikimotoi* can take up the DON produced from *P. donghaiense* and other algae to promote its own growth, according to the results of our MDON treatment experiment (Figs 4a and 6a). Field culture experimental data showed the absorption of DON and NH_4^+-N by *K. mikimotoi* in the later period (Figs 4 and 5), which might be released from the algae (Buchan et al., 2014). Many studies have also shown that *Karenia* has a competitive advantage under low nutrient concentrations (Liu, 2012), and the N/P ratio (average 4.7) is low during *Karenia* blooms (Ding and Zhang, 2018). Therefore, the nitrogen forms utilized by *Karenia* might include DIN and algal-sourced DON. Studies have shown that the bloom of *S. trochoidea* is driven not only by nutrients but also by symbiosis with other algae (Yih et al., 2004; Yin et al., 2008). This is consistent with our results that the simultaneous presence of *Karenia* spp. and *P. donghaiense* blooms in the field cruise observation (Fig. 3).

In this study, a multiprocess coupled biogeochemical model (NTPD) was used to fit the data from the field culture experiment,

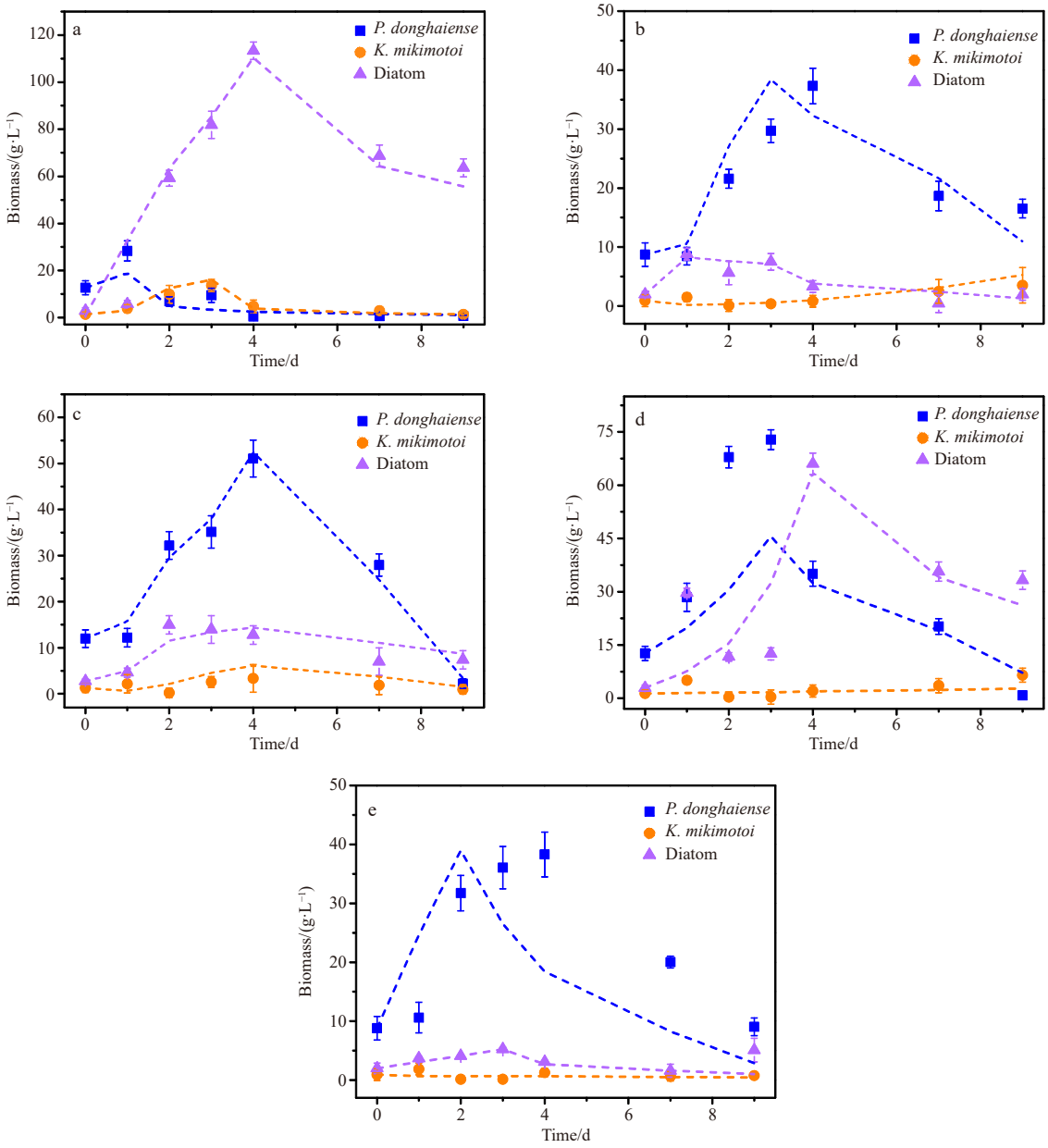

Fig. 6. Growth and death curves of three species of algae in the field culture experiments (a. MDON, b. TeDON, c. PO_4^{3-}-P, d. NO_3^--N, e. NH_4^+-N; dots represent the *in situ* concentration in the field experiment, and dash lines represent the model fitting curves).

and the key migration and transformation processes of the growth and death of *Karenia* and *P. donghaiense* were accurately revealed by combining the least squares method and Mann-Kendall method. The absorption rhythm of NO_3^--N, NH_4^+-N and DON among *Karenia*, *P. donghaiense* and diatoms in biogeochemical processes is proposed. There was competitive adsorption of DON and NH_4^+-N between diatoms and *Karenia* and competitive absorption of NO_3^--N between diatoms and *P. donghaiense* (Table 2 and Fig. 7).

The results of the NTPD model and field culture experiment showed that higher K_G with quicker addition of DIN made *P. donghaiense* more competitive than *K. mikimotoi* and diatoms, and higher K_G with quicker addition of K_{up}_DON made *K. mikimotoi* more competitive than *P. donghaiense* in ambient MDON addition or DIN exhaustion (Table 2). The absorption preference of DON and NH_4^+-N in *Karenia* is exactly consistent with the study that NH_4^+-N can inhibit the absorption and assimilation of NO_3^--N by phytoplankton (Wilkerson et al., 2006; Parker et al., 2012; Glibert et al., 2014). The diatom can take up a large amount of nutrients and thus grow rapidly (Wasmund et al., 2017), but no research has shown that diatoms can uptake the DON released by the death of other algae. Based on the field culture experiments and the NTPD model, the DIN uptake K_s of *K. mikimotoi* was higher than that of the other algae. This might induce the *K. mikimotoi* bloom to lag behind the *P. donghaiense* bloom. Diatoms are dominant competitors when DIN is abundant (Xiao et al., 2018a), while they did not become the main dominant algal species in the early stage of the field culture experiments. This might be because *P. donghaiense* was the dominant algae (75%) at the initiation point in the field cultural system, which infers that the initial algal species are also critical for the phytoplankton regime shift.

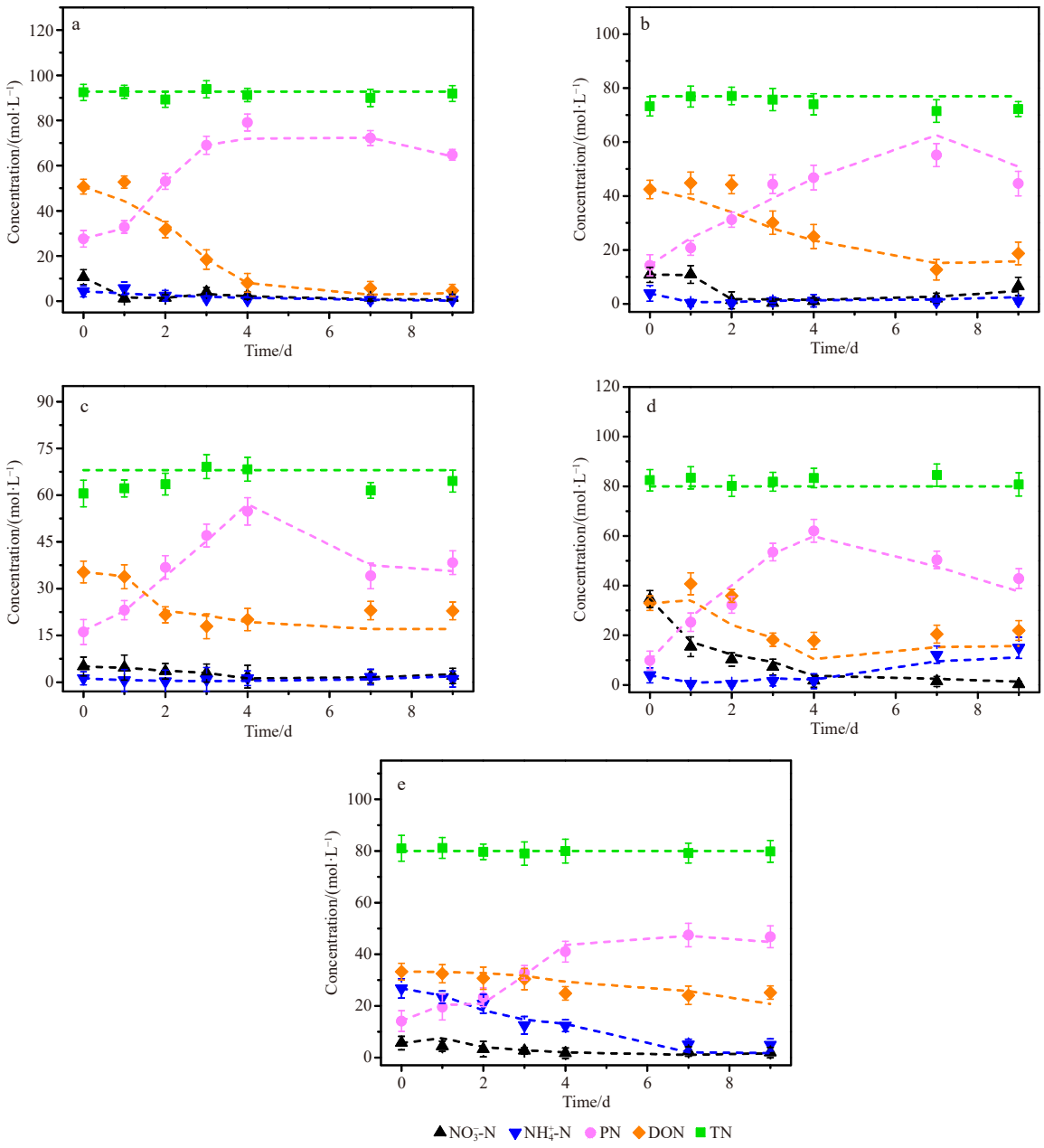

Fig. 7. Variations in nutrient concentrations in the field culture experiments (a. MDON, b. TeDON, c. PO_4^{3-}-P, d. NO_3^--N, e. NH_4^+-N; dots represent the *in situ* concentration in the field experiment, and dash lines represent the model fitting curves).

Table 2. Parameters of the NTPD model maximum growth, death, uptake of diatoms and dinoflagellates (*P. donghaiense* and *K. mikimotoi*); half-saturation constants of dissolved nitrogen of diatoms and dinoflagellates (*P. donghaiense* and *K. mikimotoi*); ammonium oxidation rate constants

Parameter	Description	Unit	*P. donghaiense*	*K. mikimotoi*	Diatom
K_G	maximum growth rate constant	d^{-1}	0.60	0.50	0.20
K_D	maximum death rate constant	d^{-1}	0.20	0.10	0.01
$K_{up}\_NH_4^+$	maximum uptake rate constants for NH_4^+-N	d^{-1}	0.40	0.10	0.20
$K_{up}\_NO_3^-$	maximum uptake rate constants for NO_3^--N	d^{-1}	0.50	0.20	0.30
K_{up}_DON	maximum uptake rate constants for DON	d^{-1}	0.075	0.30	0.18
$K_s\_NH_4^+$	half-saturation coefficients for NH_4^+-N uptake	μmol/L	0.25	0.90	0.50
$K_s\_NO_3^-$	half-saturation coefficients for NO_3^--N uptake	μmol/L	0.75	0.60	0.16
*K*s_DON	half-saturation coefficients for DON uptake	μmol/L	0.50	0.90	0.50
$KNH_4^+\_NO_3^-$	maximum ammonium oxidation rate constant	d^{-1}	0.05	0.05	0.05

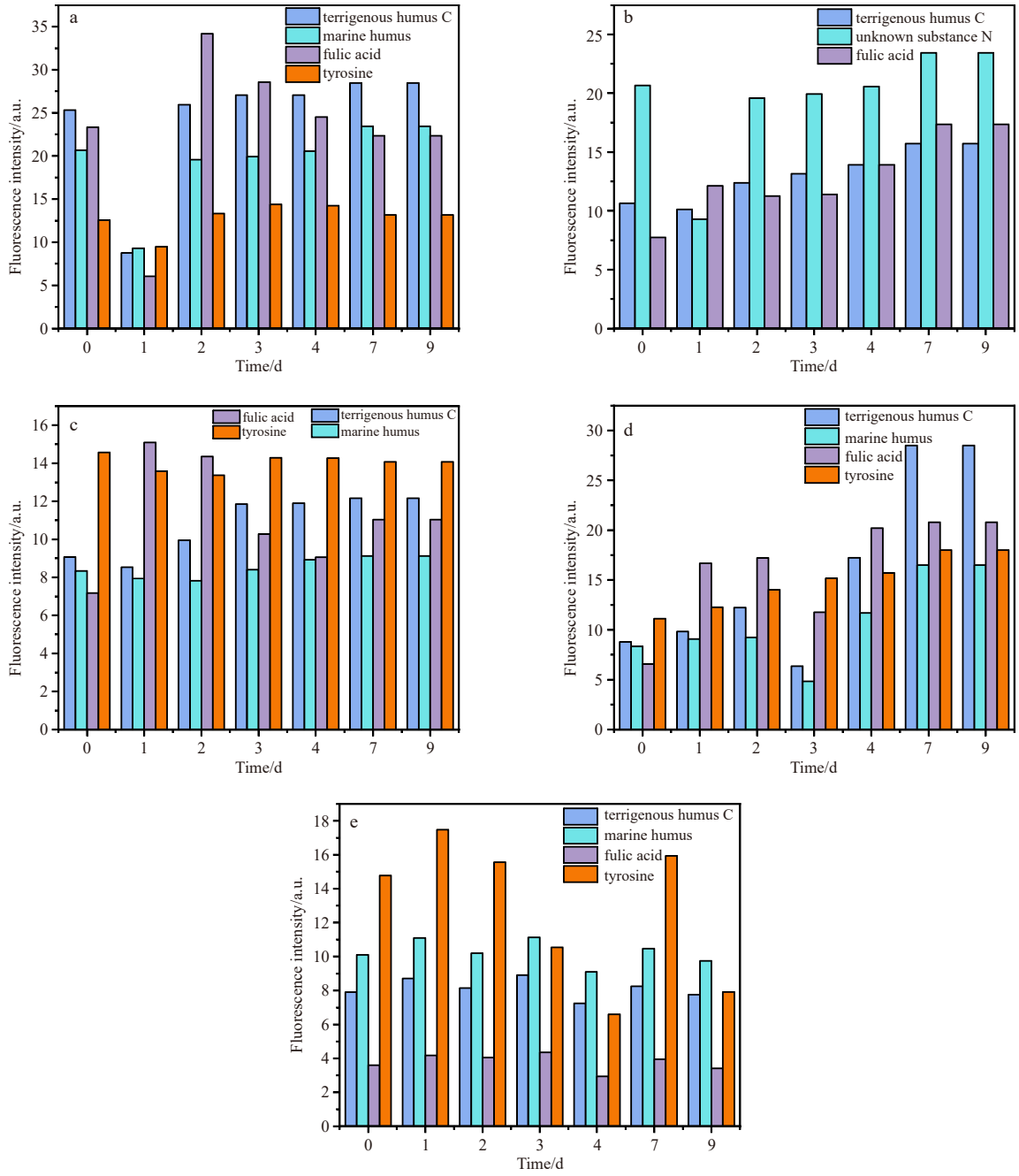

Fig. 8. Fluorescence intensity changes in five groups of enrichment experiments (a. MDON, b. TeDON, c. PO_4^{3-}-P, d. NO_3^--N, e. NH_4^+-N).

There is a synchronism rhythm of diatoms-*P. donghaiense*-*Karenia* spp.-diatom in which the phytoplankton regime shifts from diatoms to dinoflagellates of *P. donghaiense*-*Karenia* spp. loop in the East China Sea coastal waters based on field cruise observations (Fig. 10). This is consistent with the field culture experiments. In our field culture experiments, the growth of *P. donghaiense* in the condition of TeDON and DIN enrichment had advantages, while *K. mikimotoi* increased significantly in the enrichment of MDON and PO_4^{3-}-P (Fig. 6). Thus, nutrients from sewage treatment plants and aquaculture tailwater input and transport from southwest to northeast with the Taiwan Strait Current (Liu et al., 2021) promote the dinoflagellate blooms and diatom-dinoflagellate regime shifts, with the synchronism rhythm that *P. donghaiense* dominants at the loop-phase-I for the ambient eutrophic DIN and TeDON, whereas *Karenia* spp. dominant at the loop-phase-II for the exhaust of DIN and MDON released from *P. donghaiense* in the coastal waters of the East China Sea (Fig. 10).

4.2 *Triggering effect of dissolved organic matter components on dinoflagellate blooms*

Fluorescence analysis of CDOM has been widely used in algal bloom studies. CDOM is a component of dissolved organic carbon (DOC), which mainly absorbs blue and ultraviolet radiation and affects coastal primary production (Nielsen and Ekelund, 1993; Carlsson et al., 1995; Massi et al., 2020). Diatoms, cyanobacteria and green algae can be classified accurately by three-dimensional fluorescence analysis (Lv et al., 2005; Yin et al., 2014; Zhao et al., 2018). Nitrogen-containing organic compounds in seawater in this study may have different degrees of

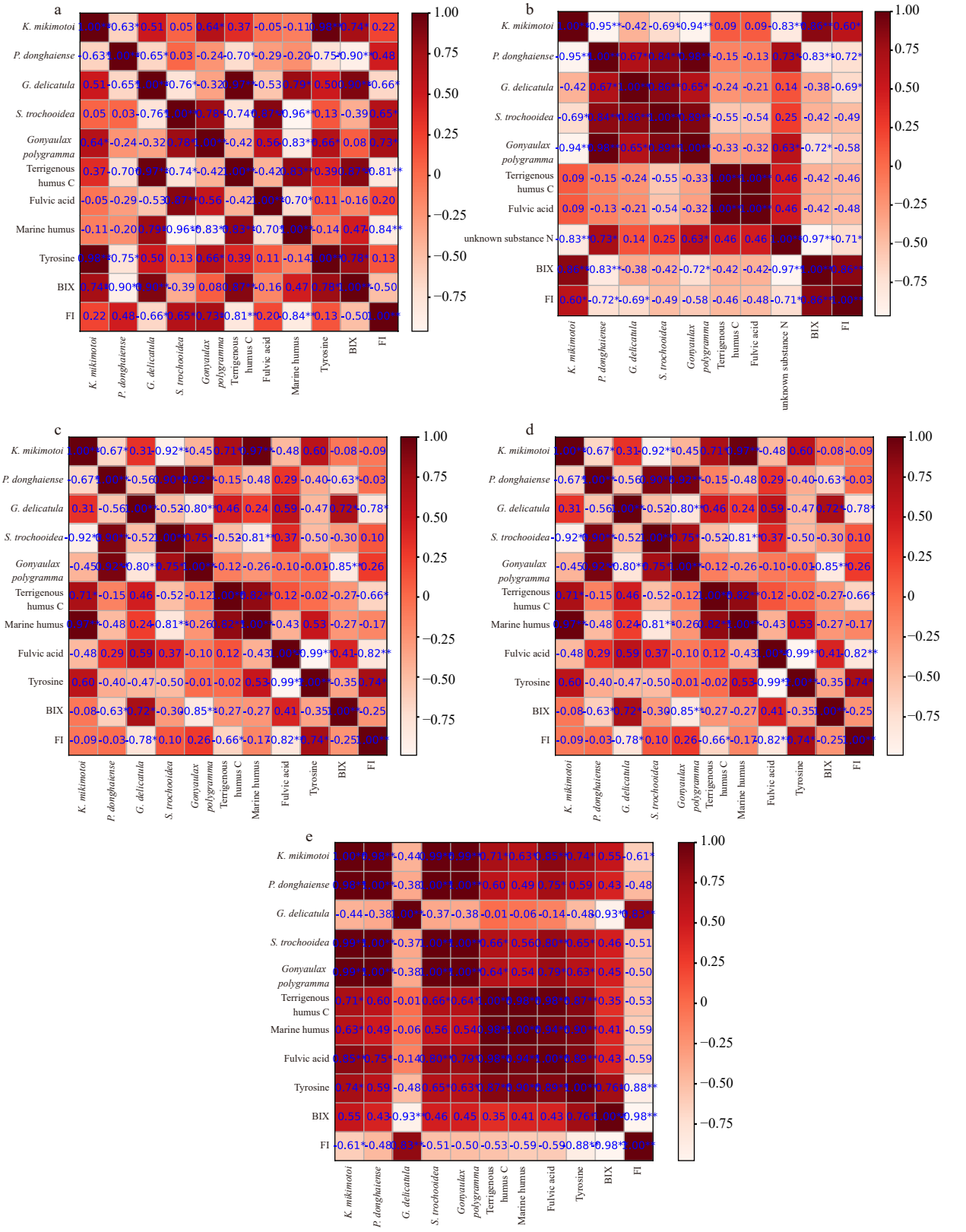

Fig. 9. Correlation analysis between CDOM and phytoplankton (a. MDON, b. TeDON, c. PO_4^{3-}-P, d. NO_3^--N, e. NH_4^+-N; +: positive correlation; –: negative correlation). Color code represents correlation coefficient.

bioavailability, so it is important to further characterize this DON component. The absorption and utilization of DON components by phytoplankton can be understood through the analysis of the process of absorption, degradation, release and transformation of DOM by phytoplankton. Therefore, CDOM is considered to be one of the main characteristics of phytoplankton (Massi et al., 2020). Then, other phytoplankton processes, such as excretion/death, perhaps play an important role in the production of

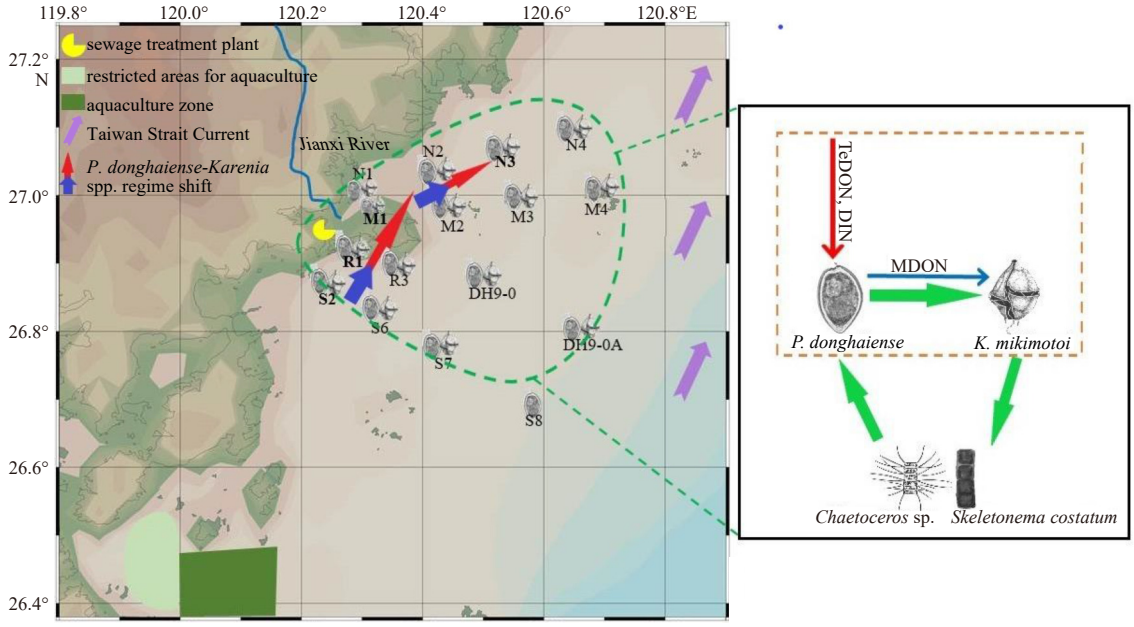

Fig. 10. The mechanism diagram of *Prorocentrum donghaiense* and *Karenia* spp. blooms. Nutrients are discharged from sewage treatment plants and aquaculture tailwater and transported from southwest to northeast with the Taiwan Strait Current, which promotes the dinoflagellate blooms and diatom-dinoflagellate regime shifts. The dinoflagellate regime shift loop is *P. donghaiense* dominant in phase Ⅰ for the ambient eutrophic DIN and TeDON, whereas *Karenia* spp. was dominant in phase Ⅱ for the exhaust of DIN and MDON released from *P. donghaiense* in the coastal waters of the East China Sea.

CDOM. Despite this, the role of phytoplankton in CDOM generation and the relationship between different algae and humus and amino acids remain unclear.

Therefore, the three-dimensional fluorescence spectrum data of field observation stations and nutrient enrichment experiments were analyzed based on parallel factor analysis. The results showed that there were three or four kinds of CDOM in all samples (Fig. 8). The correlation between DOC and FI was inversely proportional (Fig. S6). Combined with the BIX index and fluorescence intensity, it was found that the CDOM content was conducive to indicating algal blooms (Park et al., 2022). The fluorescence intensity of fulvic acid changed obviously, which has a good correlation with the biomass of *Karenia* spp. in coastal water (Fig. S7). There was a quantitative relationship between the fluorescence components of terrestrial humus C and tyrosine and the growth of *P. donghaiense* (Fig. S7). The blooms of *P. donghaiense* and *Karenia* spp. were synchronized, so the changes in the intensity of CDOM also reflected the changes in the number of the two dinoflagellates. This is consistent with the results of field culture experiments. Thus, the fluorescence components of fulvic acid, terrestrial humus C and tyrosine might be used as biomarkers of *Karenia* spp. and *P. donghaiense* in the East China Sea.

5 Conclusions

In this study, a multinitrogen-tri-phytoplankton-detritus model was built based on field cruise observations and field mesocosm flask culture experiments. According to the results of field culture experiments, there is a synchronism rhythm of the diatom-*P. donghaiense*-*Karenia* spp.-diatom loop in East China Sea coastal waters. This is consistent with the results of field cruise observations. This study infers that the *P. donghaiense* and *Karenia* spp. regime shift mechanism is associated with the nitrogen forms, where TeDON and DIN promote *P. donghaiense*, while MDON promotes *Karenia* spp. in the coastal waters of the East China Sea. The growth and nutrient uptake kinetics and the three-dimensional fluorescence characteristic of CDOM proved the triggering effect of DON on the shift of *P. donghaiense* to *Karenia* spp. TeDON with characteristics of terrestrial humus C and tyrosine components promoted the growth processes of *P. donghaiense*, while MDON from *P. donghaiense* with fulvic acid components promoted the growth processes of *Karenia* spp.

Acknowledgements

We thank to Yulan Zeng from the Second Institute of Oceanography, Ministry of Natural Resources for providing the data of algae from the field investigation.

References

An Xinlong, Li Xuemei, Yao Qiang. 2011. Two new recorded species of *Alexandrium tamarense* in Hebei Province-*Karenia mikimotoi* Hansen and *Protoperidinium leonis* Balech. Journal of Anhui Agricultural Sciences (in Chinese), 39(2): 631

Anderson D M, Glibert P M, Burkholder J M. 2002. Harmful algal blooms and eutrophication: nutrient sources, composition, and consequences. Estuaries, 25(4): 704–726, doi: 10.1007/BF02804901

Antia N J, Harrison P J, Oliveira L. 1991. The role of dissolved organic nitrogen in phytoplankton nutrition, cell biology and ecology. Phycologia, 30(1): 1–89, doi: 10.2216/i0031-8884-30-1-1.1

Boyer J N, Kelble C R, Ortner P B, et al. 2009. Phytoplankton bloom status: Chlorophyll *a* biomass as an indicator of water quality condition in the southern estuaries of Florida, USA. Ecological Indicators, 9(6): S56–S67, doi: 10.1016/j.ecolind.2008.11.013

Brand L E, Compton A. 2007. Long-term increase in *Karenia brevis* abundance along the Southwest Florida Coast. Harmful Algae, 6(2): 232–252, doi: 10.1016/j.hal.2006.08.005

Buchan A, LeCleir G R, Gulvik C A, et al. 2014. Master recyclers: Features and functions of bacteria associated with phytoplankton blooms. Nature Reviews Microbiology, 12(10): 686–698, doi: 10.1038/nrmicro3326

Carlsson P, Granéli E, Tester P, et al. 1995. Influences of riverine humic substances on bacteria, protozoa, phytoplankton, and copepods in a coastal plankton community. Marine Ecology Progress Series, 127: 213–221, doi: 10.3354/meps127213

Cen Jingyi, Wang Jianyan, Huang Lifen, et al. 2020. Who is the "murderer" of the bloom in coastal waters of Fujian, China, in 2019?. Journal of Oceanology and Limnology, 38(3): 722–732, doi: 10.1007/s00343-019-9178-6

Chen Kan, Li Keqiang, Gao Peiyi, et al. 2022. Was dissolved nitrogen regime driving diatom to dinoflagellate shift in the Bohai Sea? Evidences from microcosm experiment and modeling reproduction. Journal of Geophysical Research: Biogeosciences, 127(6): e2021JG006737, doi: 10.1029/2021JG006737

Chen Baohong, Wang Kang, Guo Huige, et al. 2021. *Karenia mikimotoi* blooms in coastal waters of China from 1998 to 2017. Estuarine, Coastal and Shelf Science, 249: 107034, doi: 10.1016/j.ecss.2020.107034

Ding Guangmao, Zhang Shufeng. 2018. Ecological characteristics and the causes of *Karenia mikimotoi* bloom in the Sansha Bay in 2012. Haiyang Xuebao (in Chinese), 40(6): 104–112, doi: 10.3969/j.issn.0253-4193.2018.06.010

Fujian Provincial Department of Ocean and Fisheries. 2019. Fujian's Ocean Disaster Report, http://hyyyj.fujian.gov.cn/(in Chinese [2020-09-07/2022-06-21])

Glibert P M, Burkholder M J. 2011. Harmful algal blooms and eutrophication: "strategies" for nutrient uptake and growth outside the Redfield comfort zone. Chinese Journal of Oceanology and Limnology, 29(4): 724–738, doi: 10.1007/s00343-011-0502-z

Glibert P M, Wilkerson F P, Dugdale R C, et al. 2014. Phytoplankton communities from San Francisco Bay Delta respond differently to oxidized and reduced nitrogen substrates-even under conditions that would otherwise suggest nitrogen sufficiency. Frontiers in Marine Science, 1: 17, doi: 10.3389/fmars.2014.00017

Harrison P J, Furuya K, Glibert P M, et al. 2011. Geographical distribution of red and green *Noctiluca scintillans*. Chinese Journal of Oceanology and Limnology, 29(4): 807–831, doi: 10.1007/s00343-011-0510-z

Heil C A, Dixon L K, Hall E, et al. 2014. Blooms of *Karenia brevis* (Davis) G. Hansen & Ø. Moestrup on the West Florida Shelf: Nutrient sources and potential management strategies based on a multi-year regional study. Harmful Algae, 38: 127–140, doi: 10.1016/j.hal.2014.07.016

Heisler J, Glibert P M, Burkholder J M, et al. 2008. Eutrophication and harmful algal blooms: A scientific consensus. Harmful Algae, 8(1): 3–13, doi: 10.1016/j.hal.2008.08.006

Hu Chuanmin, Muller-Karger F E, Swarzenski P W. 2006. Hurricanes, submarine groundwater discharge, and Florida's red tides. Geophysical Research Letters, 33(11): L11601, doi: 10.1029/2005GL025449

Huang Bangqin, Ou Linjian, Hong Huasheng, et al. 2005. Bioavailability of dissolved organic phosphorus compounds to typical harmful dinoflagellate *Prorocentrum donghaiense* Lu. Marine Pollution Bulletin, 51(8–12): 838–844, doi: 10.1016/j.marpolbul.2005.02.035

Huang C, Qi Y. 1997. The abundance cycle and influence factors on red tide phenomena of *Noctiluca scintillans* (Dinophyceae) in Dapeng Bay, the South China Sea. Journal of Plankton Research, 19(3): 303–318, doi: 10.1093/plankt/19.3.303

Imai I, Yamaguchi M, Hori Y. 2006. Eutrophication and occurrences of harmful algal blooms in the Seto Inland Sea, Japan. Plankton and Benthos Research, 1(2): 71–84, doi: 10.3800/pbr.1.71

Jeong H J, Lim A S, Lee K, et al. 2017. Ichthyotoxic *Cochlodinium polykrikoides* red tides offshore in the South Sea, Korea in 2014: I. Temporal variations in three-dimensional distributions of red-tide organisms and environmental factors. Algae, 32(2): 101–130, doi: 10.4490/algae.2017.32.5.30

Killberg-Thoreson L, Mulholland M R, Heil C A, et al. 2014. Nitrogen uptake kinetics in field populations and cultured strains of *Karenia brevis*. Harmful Algae, 38: 73–85, doi: 10.1016/j.hal.2014.04.008

Kwon H K, Kim G, Han Yongjin, et al. 2019. Tracing the sources of nutrients fueling dinoflagellate red tides occurring along the coast of Korea using radium isotopes. Scientific Reports, 9(1): 15319, doi: 10.1038/s41598-019-51623-w

Lai Junxiang, Yu Zhiming, Song Xiuxian, et al. 2011. Responses of the growth and biochemical composition of *Prorocentrum donghaiense* to different nitrogen and phosphorus concentrations. Journal of Experimental Marine Biology and Ecology, 405(1–2): 6–17, doi: 10.1016/j.jembe.2011.05.010

Li Xiaodong, Yan Tian, Yu Rencheng, et al. 2019. A review of *Karenia mikimotoi*: Bloom events, physiology, toxicity and toxic mechanism. Harmful Algae, 90: 101702, doi: 10.1016/j.hal.2019.101702

Lin Jianing, Yan Tian, Zhang Qingchun, et al. 2014. *In situ* detrimental impacts of *Prorocentrum donghaiense* blooms on zooplankton in the East China Sea. Marine Pollution Bulletin, 88(1–2): 302–310, doi: 10.1016/j.marpolbul.2014.08.026

Lin Jianing, Yan Tian, Zhang Qingchun, et al. 2016. Impact of several harmful algal bloom (HAB) causing species, on life history characteristics of rotifer *Brachionus plicatilis* Müller. Chinese Journal of Oceanology and Limnology, 34(4): 642–653, doi: 10.1007/s00343-016-5065-6

Liu Chunqiang. 2012. Effects of nutrient on the community succession of six marine microalgae (in Chinese)[dissertation]. Qingdao: Ocean University of China

Liu Zhiqiang, Gan Jianping, Hu Jianyu, et al. 2021. Progress on circulation dynamics in the East China Sea and southern Yellow Sea: Origination, pathways, and destinations of shelf currents. Progress in Oceanography, 193: 102553, doi: 10.1016/j.pocean.2021.102553

Liu Gang, Janowitz G S, Kamykowski D. 2001. A biophysical model of population dynamics of the autotrophic dinoflagellate *Gymnodinium breve*. Marine Ecology Progress Series, 210: 101–124, doi: 10.3354/meps210101

Long Hua, Du Qi, 2005. Primary research on *Karenia mikimotoi* bloom in Fujian coast. Journal of Fisheries Research (in Chinese), (4): 22–26, doi: 10.14012/j.cnki.fjsc.2005.04.006

Lv Songhui, Cen Jingyi, Wang Jianyan, et al. 2019. The research status quo, hazard, and ecological mechanisms of *Karenia mikimotoi* red tide in coastal waters of China. Oceanologia et Limnologia Sinica (in Chinese), 50(3): 487–494, doi: 10.11693/hyhz20181000255

Lv Honggang, Zhang Xihui, Gong Chunying, et al. 2005. Studies on the algorithm and identification of three dimensional fluorescence spectroscopy of algae. China Environmental Science (in Chinese), 25(5): 581–584

Marques A C, Veras C E, Kumpel E, et al. 2024. Assessment of nutrients and conductivity in the Wachusett Reservoir watershed: An investigation of land use contributions and trends. International Soil and Water Conservation Research, 12(2): 337–350, doi: 10.1016/j.iswcr.2023.07.004

Massi L, Frittitta L, Melillo C, et al. 2020. Seasonal dynamic of CDOM in a shelf site of the South-Eastern Ligurian sea (Western Mediterranean). Journal of Marine Science and Engineering, 8(9): 703, doi: 10.3390/jmse8090703

Mathew T, Prakash S, Baliarsingh S K, et al. 2021. Response of phytoplankton biomass to nutrient stoichiometry in coastal waters of the western Bay of Bengal. Ecological Indicators, 131: 108119, doi: 10.1016/j.ecolind.2021.108119

Medina M, Huffaker R, Jawitz J W, et al. 2020. Seasonal dynamics of terrestrially sourced nitrogen influenced *Karenia brevis* blooms off Florida's southern gulf coast. Harmful Algae, 98: 101900, doi: 10.1016/j.hal.2020.101900

Mulholland M R, Bernhardt P W, Heil C A, et al. 2006. Nitrogen fixation and release of fixed nitrogen by *Trichodesmium* spp. in the Gulf of Mexico. Limnology and Oceanography, 51(4): 1762–1776, doi: 10.4319/lo.2006.51.4.1762

Nielsen T, Ekelund N G A. 1993. Effect of UV-B radiation and humic substances on growth and motility of *Gyrodinium aureolum*. Limnology and Oceanography, 38(7): 1570–1575, doi: 10.4319/lo.1993.38.7.1570

O'Neil J M, Heil C A. 2014. Nutrient dynamics of *Karenia brevis* red

tide blooms in the eastern Gulf of Mexico. Harmful Algae, 38: 1–140, doi: 10.1016/j.hal.2014.08.004

Park J, Kim G, Kwon H K, et al. 2022. Origins and characteristics of dissolved organic matter fueling harmful dinoflagellate blooms revealed by δ^{13}C and D/L-Amino acid compositions. Scientific Reports, 12(1): 15052, doi: 10.1038/s41598-022-19168-7

Parker A E, Hogue V E, Wilkerson F P, et al. 2012. The effect of inorganic nitrogen speciation on primary production in the San Francisco Estuary. Estuarine, Coastal and Shelf Science, 104–105: 91–101, doi: 10.1016/j.ecss.2012.04.001

Parsons T R, Maita Y, Lalli C M. 1984. Determination of chlorophylls and total carotenoids: spectrophotometric method. In: Parsons T R, Maita Y, Lalli C M, eds. A Manual of Chemical & Biological Methods for Seawater Analysis. Amsterdam: Elsevier, 101–104, doi: 10.1016/B978-0-08-030287-4.50032-3

Stedmon C A, Bro R. 2008. Characterizing dissolved organic matter fluorescence with parallel factor analysis: a tutorial. Limnology and Oceanography: Methods, 6(11): 572–579, doi: 10.4319/lom.2008.6.572

Steidinger K A. 2009. Historical perspective on *Karenia brevis* red tide research in the Gulf of Mexico. Harmful Algae, 8(4): 549–561, doi: 10.1016/j.hal.2008.11.009

Strickland J D H, Parsons T R. 1970. A Practical Handbook of Seawater Analysis. Ottawa: Fisheries Research Board of Canada, doi: 10.1002/iroh.19700550118

Tester P A, Shea D, Kibler S R, et al. 2008. Relationships among water column toxins, cell abundance and chlorophyll concentrations during *Karenia brevis* blooms. Continental Shelf Research, 28(1): 59–72, doi: 10.1016/j.csr.2007.04.007

Tilney C L, Shankar S, Hubbard K A, et al. 2019. Is *Karenia brevis* really a low-light-adapted species?. Harmful Algae, 90: 101709, doi: 10.1016/j.hal.2019.101709

van de Poll W H, Kulk G, Timmermans K R, et al. 2013. Phytoplankton chlorophyll *a* biomass, composition, and productivity along a temperature and stratification gradient in the northeast Atlantic Ocean. Biogeosciences, 10(6): 4227–4240, doi: 10.5194/bg-10-4227-2013

Vargo G A, Heil C A, Fanning K A, et al. 2008. Nutrient availability in support of *Karenia brevis* blooms on the central West Florida Shelf: what keeps *Karenia* blooming?. Continental Shelf Research, 28(1): 73–98, doi: 10.1016/j.csr.2007.04.008

Wang Xuejing. 2015. Effects of urea on the growth of typical algae in the East China Sea (in Chinese)[dissertation]. Qingdao: Ocean University of China

Wang Yan, Liu Yongjian, Guo Hao, et al. 2022. Long-term nutrient variation trends and their potential impact on phytoplankton in the southern Yellow Sea, China. Acta Oceanologica Sinica, 41(6): 54–67, doi: 10.1007/s13131-022-2031-3

Wang Yujue, Liu Dongyan, Xiao Wupeng, et al. 2021. Coastal eutrophication in China: trend, sources, and ecological effects. Harmful Algae, 107: 102058, doi: 10.1016/j.hal.2021.102058

Wang Jinhui, Qin Yutao, Liu Caicai, et al. 2006. The preliminary investigation of potentially toxic algae and bio-toxin in Changjiang Estuary. Marine Environmental Science (in Chinese), 25(S1): 52–61

Wasmund N, Kownacka J, Göbel J, et al. 2017. The diatom/dinoflagellate index as an indicator of ecosystem changes in the Baltic Sea 1. Principle and handling instruction. Frontiers in Marine Science, 4: 22, doi: 10.3389/fmars.2017.00022

Wilkerson F P, Dugdale R C, Hogue V E, et al. 2006. Phytoplankton blooms and nitrogen productivity in San Francisco Bay. Estuaries and Coasts, 29(3): 401–416, doi: 10.1007/BF02784989

Xia Wei. 2016. Study on molecular response mechanism of *Prorocentrum donghaiense* Lu and *Karenia mikimotoi* Hansen grown into nitrogen limitation or phosphorus limitation (in Chinese)[dissertation]. Guangzhou: Jinan University

Xiao Xi, Agustí S, Pan Yaoru, et al. 2019. Warming amplifies the frequency of harmful algal blooms with eutrophication in Chinese coastal waters. Environmental Science & Technology, 53(22): 13031–13041, doi: 10.1021/acs.est.9b03726

Xiao Wupeng, Liu Xin, Irwin A J, et al. 2018a. Warming and eutrophication combine to restructure diatoms and dinoflagellates. Water Research, 128: 206–216, doi: 10.1016/j.watres.2017.10.051

Xiao Wupeng, Wang Lei, Laws E, et al. 2018b. Realized niches explain spatial gradients in seasonal abundance of phytoplankton groups in the South China Sea. Progress in Oceanography, 162: 223–239, doi: 10.1016/j.pocean.2018.03.008

Yan Tian, Zhou Mingjiang. 2004. Environmental and health effects associated with Harmful Algal Bloom and marine algal toxins in China. Biomedical and Environmental Sciences, 17(2): 165–176

Yao Weimin, Pan Xiaodong, Hua Dandan. 2007. A preliminary study on the origin of red tide of *Karenia mikimotoi* in Zhejiang waters. Reservoir Fisheries (in Chinese), 27(6): 57–58,76

Yih W, Kim H S, Jeong H J, et al. 2004. Ingestion of cryptophyte cells by the marine photosynthetic ciliate *Mesodinium rubrum*. Aquatic Microbial Ecology, 36(2): 165–170, doi: 10.3354/ame036165

Yin Kedong, Song Xiuxian, Liu Sheng, et al. 2008. Is inorganic nutrient enrichment a driving force for the formation of red tides? A case study of the dinoflagellate *Scrippsiella trochoidea* in an embayment. Harmful Algae, 8(1): 54–59, doi: 10.1016/J.HAL.2008.08.004

Yin Gaofang, Zhao Nanjing, Hu Li, et al. 2014. Classified measurement of Phytoplankton based on characteristic fluorescence of photosynthetic pigments. Acta Optica Sinica (in Chinese), 34(9): 0930005, doi: 10.3788/AOS201434.0930005

Zhang Jinfeng, Gao Xuelu, Li Peimiao, et al. 2015. Nutrient distribution characteristics and long-term trends in the southwest of the Laizhou Bay and its adjacent rivers. Marine Science Bulletin (in Chinese), 34(2): 222–232, doi: 10.11840/j.issn.1001-6392.2015.02.015

Zhang Xiansheng, Zhen Guangming, Cui Xiaoru, et al. 2023. Effect of dissolved organic nutrients on the bloom of *Prorocentrum donghaiense* in the East China Sea coastal waters. Marine Environmental Research, 183: 105841, doi: 10.1016/j.marenvres.2022.105841

Zhao Congjiao, Liu Xizhen, Fu Shengjing, et al. 2020. Variation characteristics of the evolution of *Karenia mikimotoi* bloom and environmental factors based on online monitoring buoy data. Journal of Tropical Oceanography (in Chinese), 39(2): 88–97, doi: 10.11978/2019027

Zhao Yanmin, Qin Yanwen, Zhang Lei, et al. 2021. Temporal and spatial distribution of red tides in the Chang-jiang Estuary and in adjacent waters from 1989 to 2019. Marine Sciences (in Chinese), 45(12): 39–46, doi: 10.11759/hykx20210220001

Zhao Nanjing, Zhang Xiaoling, Yin Gaofang, et al. 2018. On-line analysis of algae in water by discrete three-dimensional fluorescence spectroscopy. Optics Express, 26(6): A251–A259, doi: 10.1364/OE.26.00A251

Zhou Mingjiang, Shen Zhiliang, Yu Rencheng. 2008. Responses of a coastal phytoplankton community to increased nutrient input from the Changjiang (Yangtze) River. Continental Shelf Research, 28(12): 1483–1489, doi: 10.1016/j.csr.2007.02.009

Zhou Weihua, Yin Kedong, Zhu Dedi. 2006. Phytoplankton biomass and high frequency of *Prorocentrum donghaiense* harmful algal bloom in Zhoushan sea area in spring. Chinese Journal of Applied Ecology (in Chinese), 17(5): 887–893

Supplementary information:

Fig. S1. Changes in environmental factors in the field cruise observation.

Fig. S2. Changes of Chl *a* in the field cruise observation.

Fig. S3. Changes in nutrients in the field cruise observation.

Fig. S4. RDA analysis of nutrient and environmental factors in the field cruise observation. Three morphological changed of phosphorus in field culture experiment.

Fig. S5. Concentration changes of different P forms in the field culture experiment (a. MDON, b. TeDON, c. PO_4^{3-}-P, d. NO_3^--N, e. NH_4^+-N , f. control group).

Fig. S6. BIX index change diagram of five groups in the field culture experiments (a. MDON, b. TeDON, c. PO_4^{3-}-P, d. NO_3^--N, e. NH_4^+-N).

Fig. S7. Fluorescence intensity changes at three stations of N3, R1 and M1.

Fig. S8. Changes of fluorescence components in seawater at field observation stations of N3(a), R1(b) and M1(c) (contour diagram).

Table S1. Parameters of NTPD model.

Table S2. Phytoplankton identification results.

The supplementary information is available online at https://doi.org/10.1007/s13131-023-2308-9 and http://www.aosocean.com/. The supplementary information is published as submitted, without typesetting or editing. The responsibility for scientific accuracy and content remains entirely with the authors..